www.czasopisma.pan.pl PAN www.journals.pan.pl

ARCHIVES of FOUNDRY ENGINEERING

ISSN (2299-2944)
Volume 2020
Issue 1/2020

73 – 78

10.24425/afe.2020.131286

13/1

Published quarterly as the organ of the Foundry Commission of the Polish Academy of Sciences

# Analysis of Ballistic Resistance of Composites with EN AW-7075 Matrix Reinforced with $Al_2O_3$ Particles

**A. Kurzawa *, D. Pyka, K. Jamroziak**
Wroclaw University of Science and Technology, Faculty of Mechanical Engineering,
Department of Foundry Engineering, Plastics and Automation,
Smoluchowskiego 25, 50-372 Wroclaw, Poland
* Corresponding author. E-mail address: adam.kurzawa@pwr.edu.pl

Received 11.07.2019; accepted in revised form 04.11.2019

## Abstract

The paper presents the results of experimental-numerical tests of firing at aluminum composite materials. The test materials were manufactured by pressure infiltration of porous ceramic preforms made of α-$Al_2O_3$ particles in the amount of 30% and 40% by volume. The EN AW-7075 alloy was chosen as the material matrix, and the steel 7.62×39 mm (M 43) FMJ (Full Metal Jacket) intermediate ammunition was selected for firing. In the result of the experiment, the samples were perforated with a clear difference in the muzzle diameter. The projectile with fragments caused damage to up to three reference plates placed behind the samples (witness plates) in composites with 40% of particles by volume. The mechanics of crack propagation during ballistic impacts of the projectile was characterized based on microstructure studies. Then, using numerical analysis of impact load, the examination of composite materials puncture in the ABAQUS environment was carried out. The Finite Element Method (FEM) was employed for the discretization of geometric models using Hex elements. The Johnson-Cook constitutive model describing the relationship between stress and strain in metal-ceramic composites was applied for the analyses. Numerical models were then subjected to numerical verification using smoothed particle hydrodynamics (SPH). Based on the obtained results, it was found that the hybrid FEM/SPH method correlates significantly with the experimental results.

**Keywords:** Composite materials, Ballistic resistance, Finite element method (FEM), Smoothed particle hydrodynamics (SPH)

## 1. Introduction

Composite materials made of light alloys with the addition of a strengthening phase in the form of ceramic elements are coming into widespread use in the construction of machines and elements of shields protecting against impulse load. One of such solutions is multilayer composite ballistic shields [1-3]. In those systems, ceramic plates provide the best possible protection while minimizing mass and thickness. Materials such as an aluminum oxide ($Al_2O_3$), silicon carbide (SiC) and boron carbide ($B_4C$), as well as titanium boride ($TiB_2$), aluminum nitride (AlN) and silicon nitride ($Si_3N_4$)) are applied in the solutions of structures dissipating impact energies at ballistic speeds. Currently, composites with $Al_2O_3/TiB_2$ or ZTA (aluminum oxide reinforced with zirconium oxide particles) matrices are becoming popular materials. That is related to the search for better mechanical properties, especially the improvement of the resistance to brittle cracking. The paper [4, 5] describes $Al_2O_3$ materials made in the lanxide process, in which controlled oxidation of liquid aluminum

is used to create $Al_2O_3$ matrix with residual aluminum and additional ceramic particles or fibers.

The paper [6] shows that ceramic matrix composites (CMCs) have the highest potential for production of ceramic composites in applications with high temperatures, aggressive environment, chemical degradation, or abrasive loads. The total amount of products made of ceramic composite materials will steadily increase [7], and the method of liquid silicon infiltration (LSI) has the potential to produce cost-effective ceramic composites. There are few publications on CMC fiber reinforcement for impact protection in the literature. Glass reinforced with SiC fibers is presented in [8], where it has been shown that the strengthening of SiC fiber has modified the fracture properties. The paper [9] presents a monolithic ceramic material based on silicon nitride/hexagonal boron nitride ($Si_3N_4$/BN). The material was created from the fibrous texture with conventional polycrystalline hardened ceramic materials. The material was shot with a Russian anti-tank 7.62×39mm API projectile. In the works [10-12] the impact resistance of newly developed metal-ceramic composites with aluminum matrix to indirect ammunition fire of 5.56×45 mm NATO (SS109) was investigated. The composite material produced by squeeze casting method was based on AC-44200 alloy reinforced with $Al_2O_3$ preforms. CMCs with 20% and 40% vol. of $Al_2O_3$ particles were analyzed in relation to the material of the unfortified matrix. In-depth analyses of CMCs have been presented in studies [13, 14], which aimed to improve mechanical properties. The recognition of the destruction mechanism in the low and high velocities range may result in the creation of an optimal material exceeding the behavior of ceramics resulting from ballistic impact.

The authors of this paper focused on the study of ballistic resistance of composites with EN AW-7075 matrix reinforced with α-$Al_2O_3$ particles. This objective was achieved through hybrid numerical methods using FEM and SPH. The impulse load analysis was related to the impact load of the composite material with a 7.62x39 mm (M 43) FMJ projectile. The obtained results were validated experimentally.

## 2. Materials and experimental methods

Ballistic resistance tests were carried out on cast composite materials whose matrix is reinforced by the age-hardened EN AW-7075 alloy. Ceramic preforms made of 3 to 6 μm α-$Al_2O_3$ particles were used to strengthen the materials. The preforms were characterized by open porosity and contained 30% and 40% vol. of ceramic particles, respectively. Parameters [15] play a key role in the production of infiltrated composites. The infiltration of the liquid matrix of free spaces in preforms was carried out on a hydraulic press using the squeeze casting method at the following parameters:

- the alloy temperature: 720°C,
- the temperature of the preforms 700°C,
- ironing pressure: 90÷100MPa.

The structure of composite materials after infiltration is closely related to the cellular structure of preforms, which contain regularly distributed oval-like open spaces. Figure 1 displays an example of a material structure with 40% vol. of $Al_2O_3$ particles.

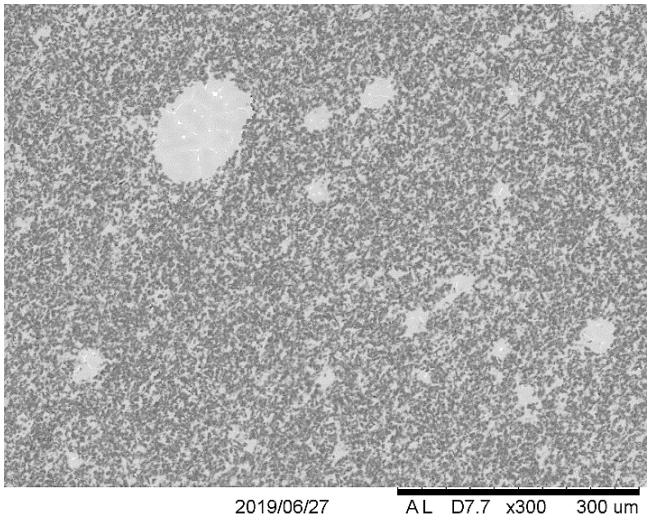


Fig. 1. Microstructure of EN AW 7075 composite material - 40% vol. of $Al_2O_3$ particles

A holder was specially designed to allow the specimen to be fixed stationary on the face side to determine the ballistic resistance of the materials. Figure 2 illustrates the view of the station.

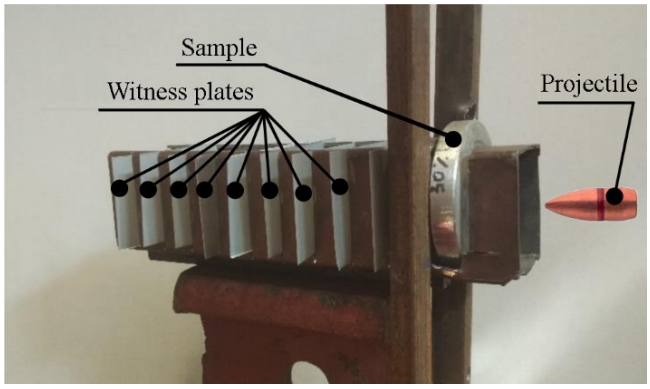


Fig. 2. Stand for firing composite materials

The value of the residual energy of the projectile after passing through the tested composite shields was estimated using ten stably embedded 0.3 m thick witness plates made of pure Al. The distance of the first reference plate from the sample and between the plates was 20 mm.

The test specimens were made in the form of discs with a diameter of 80 mm and a thickness of 12 mm. The firing of the samples was carried out on the ballistic track from the 7.62 mm AK with the 7.62×39 mm (M 43) FMJ ammunition. One projectile was fired at each specimen with the average velocity of $v_0$ =715 m/s ±10 m/s.

Numerical analysis of metal composite piercing (MMC) was performed in the ABAQUS program through the Explicit method. For this purpose, the projectile elements, the tested composite sample, and reference plates were spatially modeled (Fig. 3). 0.5 mm Hex type elements were used in the discretized model. The jacket and sabot were omitted in the numerical model of the

projectile, thereby it was simplified only to the steel core, which was given an initial velocity of 715 m/s.

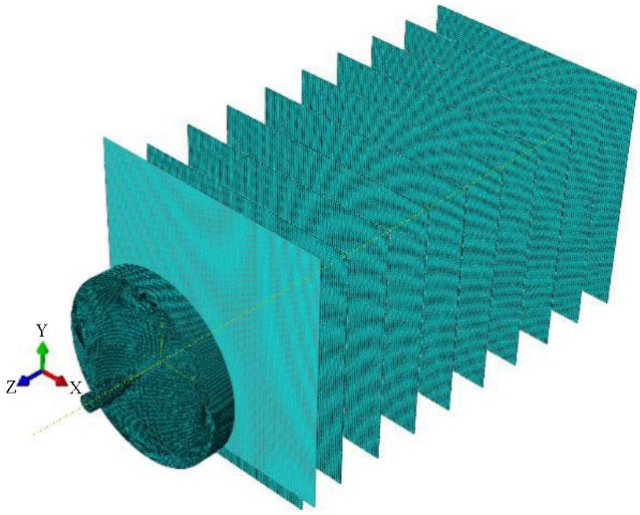


Fig. 3. Discretized model of a stand for firing composite materials

The values of mechanical properties of the tested composites, determined in separate studies by the authors of the paper, were assumed for numerical simulations (Table 1).

Table 1.
Mechanical properties of composite materials

| Materials/ Mechanical properties | EN AW7075 30% vol. $\alpha$-$Al_2O_3$ | EN AW7075 40% vol. $\alpha$-$Al_2O_3$ |
|---|---|---|
| $R_m$ [MPa] | 373 | 351 |
| $E$ [GPa] | 9910 | 9475 |
| $R_g$ [MPa] | 530 | 520 |
| $R_c$ [MPa] | 666 | 563 |
| $R_{p0.2}$ [MPa] | 478 | 448 |
| $I$ [kJ/m$^2$] | 2.5 | 2.1 |

where: $R_m$ - Tensile strength, $E$ -Young's modulus, $R_g$ - Bending strength, $R_c$ - Compressive strength, $R_{p0.2}$ - Yield strength, $I$ - Impact strength.

The Johnson-Cook plasticity model with omitting the temperature part of the equation (1) was used for mathematical description considering rheological properties of materials [16-18].

$$\sigma = (A + B\varepsilon^n)(1 + C ln\dot{\varepsilon}^*) \quad (1)$$

where: $\sigma$ is the equivalent stress, and $\varepsilon$ is the equivalent plastic strain. The material constants are $A$, $B$, $n$, and $C$. $A$ is the yield stress of the material under reference conditions, $B$ is the strain hardening constant, $n$ is the strain hardening coefficient, $C$ is the strengthening coefficient of strain rate, $\dot{\varepsilon}^*$ is the dimensionless strain rate [19].

In the numerical model describing the mechanism of destruction, the conditions of boundary deformation [20, 21] have been assumed. A hybrid method of connecting FEM algorithms with SPH was applied to avoid disturbances in the algorithm related to mass increase ($\Delta m$). It is there that after exceeding the preset destructive strain, the FEM element is converted into SPH point having the i-th mass ($m_i$)), due to which the weight in the system remains unchanged [22, 23].

The effects of firing were subjected to microscopic evaluation using the Hitachi model TM-3000 SEM electron microscope. The analysis described the mechanism of propagation of radial cracks.

# 3. Results and discussion

## 3.1. Experiment results

In the result of the firing, the projectile completely perforated the test specimens. The impact loading caused them to crack radially from the through-hole to the outside. There were usually 4 to 5 cracks (Fig. 4).

Brittle chipping of material with an average diameter of 15 mm for specimens with 30% vol. and 13 mm for those with 40% vol. of particles is produced on their surface on the side of the projectile impact. The outer hole diameter on the outlet side of the projectile is significantly influenced by the volume of particles in the composite. In samples with 30% vol. of particles, the average is 22 mm, while in ones with 40% vol. of $\alpha$-$Al_2O_3$ it is 33 mm on average (Fig. 4b).

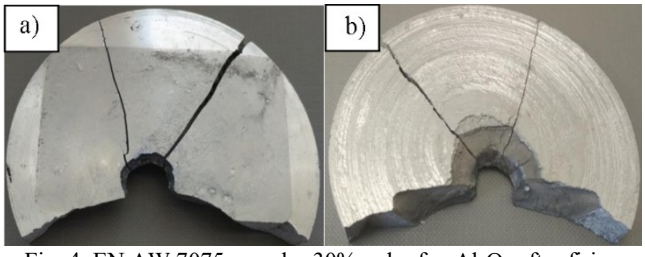


Fig. 4. EN AW 7075 sample -30% vol. of $\alpha$-$Al_2O_3$ after firing with 7.62×39 mm: a) front side, b) reverse side

The firing of composites with 30% vol. of $\alpha$-$Al_2O_3$ caused perforation of 2 plates and deformation of 2-3 reference plates. While the deformation of three witness plates without the effect of puncture occurred in composites with 40% vol. of particles.

## 3.2. Microstructure

Microscopic observations of samples in selected areas around radial cracks were implemented as part of microstructure research. The analysis showed that the development of cracks is brittle. Additional microcracks are usually formed around the main cracks, generally in the direction corresponding to the course of the main breaks (Fig. 5).

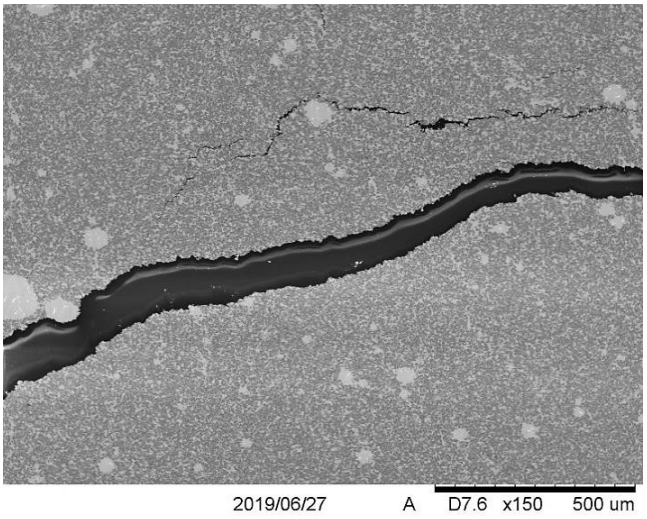


Fig. 5. View of the main cracks and additional microcracks in the composite material with 40% vol. of $\alpha$-$Al_2O_3$ particles

The areas of the matrix not filled with particles, which are present in the crack path, usually cause a change in the crack propagation direction. In this case, the crack front goes along the border with these areas (Fig. 6). Partial material fragmentation is observed along the crack edge.

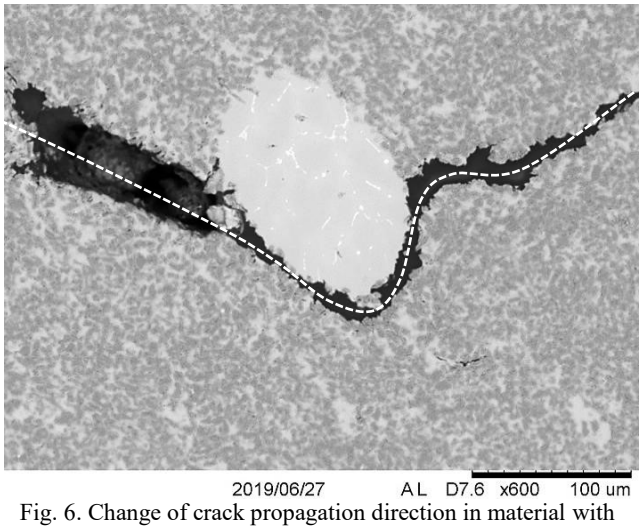


Fig. 6. Change of crack propagation direction in material with 40% vol. of $\alpha$-$Al_2O_3$ particles

Observations confirm the presence of stratification and fragmentation in materials in the areas around microcracks. Destructions of this type are the result of the most frequently occurring complex stresses causing warp deformations and particle displacement. In such places, the particles are wedged, which leads to their brittle cracking and the warp delamination from their surface (Fig. 7).

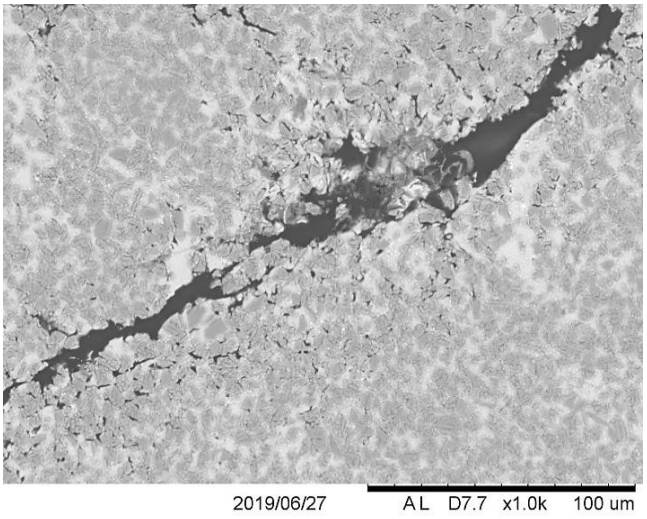


Fig. 7. Delamination and fragmentation of the matrix in the microcrack area

## 3.3. Numerical analysis

The numerical method used allowed the visualization of the perforation of composite materials, including the deformation of witness plates (Fig. 8).

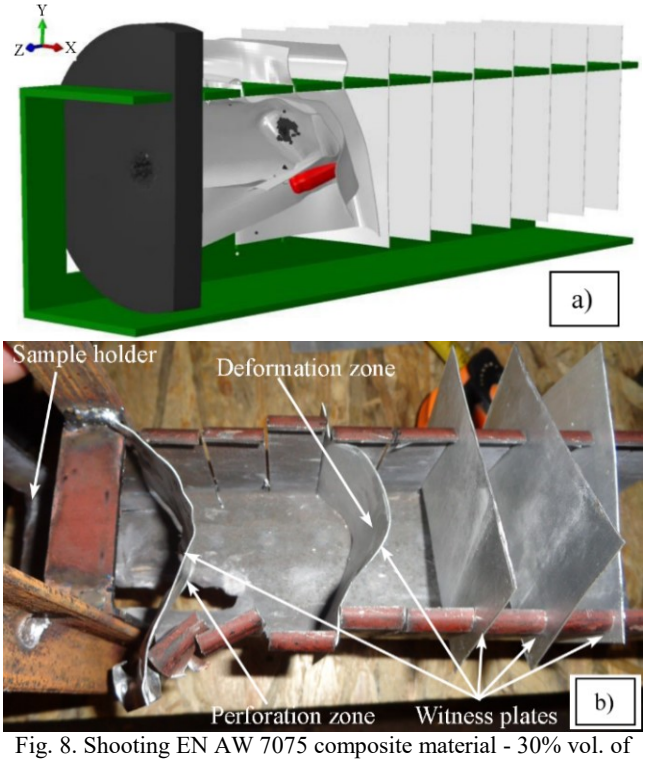


Fig. 8. Shooting EN AW 7075 composite material - 30% vol. of $\alpha$-$Al_2O_3$: a) simulation (time: 0.007 s), b) experiment

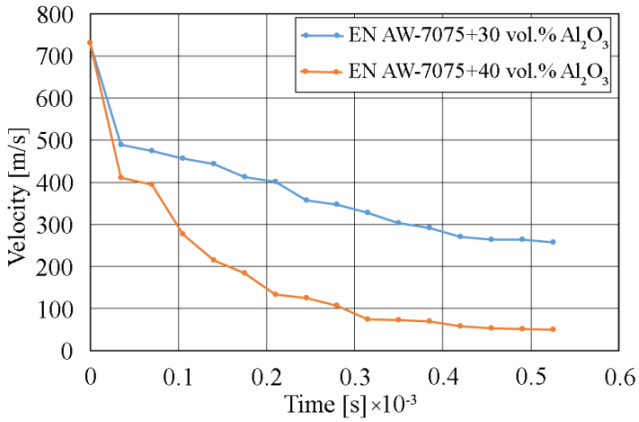


Fig. 9. Change of 7.62×39 mm projectile velocity when piercing composite materials

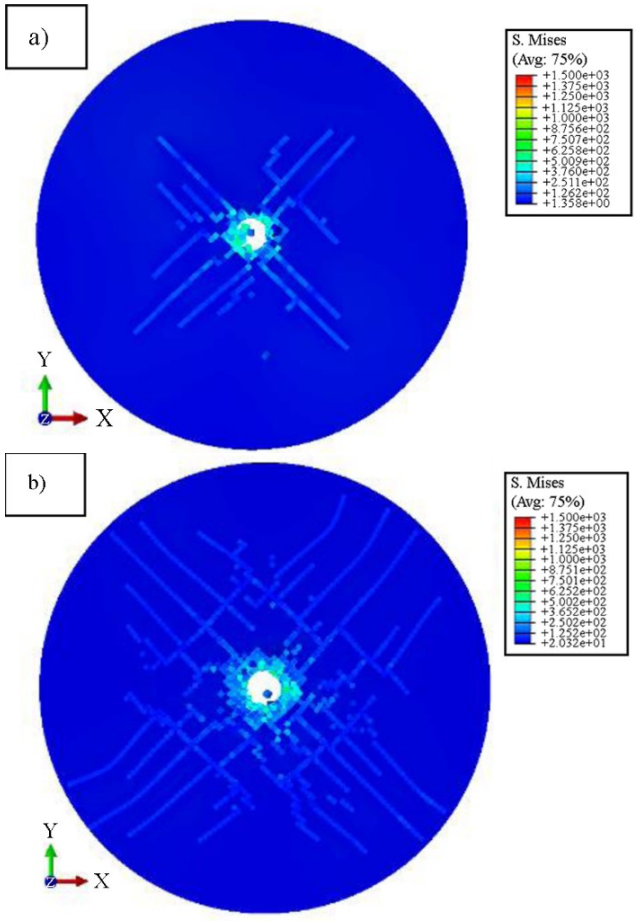


Fig. 10. Stress distribution map according to FEM numerical model of composites with: a) 30% vol. of α-$Al_2O_3$, b) 40% vol. of α-$Al_2O_3$

The visualized and experimental results are the same. During the shooting of samples with 30% vol. of particles, perforation of the first and sometimes also the second witness plate takes place. The third and fourth plates are deformed without the effect of puncture. On the other hand, the firing at samples with 40% vol. of particles does not cause perforation of witness plates but only their deformation covering the first two plates. The first aperture was perforated only in a few specimens.

The outcomes of numerical analysis are presented in the form of dependence of the projectile velocity change during the piercing of composite shields. The result is shown in Figure 9.

Figure 10 presents the effects of tests performed with the use of the FEM numerical model. As can be seen, maps of the distribution of internal stresses in the cross-section distant of 2/3 of the thickness from the surface struck by the projectile show a significant difference in stress values between the tested samples with 30% vol. and 40% vol. of α-$Al_2O_3$ particles.

The difference was 1.252e+02 MPa in favor of 40% vol. of α-$Al_2O_3$ particles. The above has been confirmed by experimental results, where there is a significant increase in the projectile outlet diameter in the specimens.

# 4. Summary and conclusions

The results of experimental and numerical ballistic resistance tests of composite materials produced based on EN AW-7075 alloy matrix confirm the effectiveness of the application of reinforcement in the form of preforms made of ceramic particles - α-$Al_2O_3$ to increase the resistance.

1. In the effect of a 7.62×39 mm projectile impact both composite materials with 30% vol. and 40% vol. of α-$Al_2O_3$ particles were perforated. The impact energy caused the formation of cracks in the composites with the direction of propagation from the through-hole, through the radius to the outside with a significant increase in the outlet diameter observed for materials with 40% vol. of reinforcing particles. In the result of the puncture, only 2 to 3 witness plates with a thickness of 0.3 m were damaged (deflection), which indicates relatively low residual energy.

2. From microstructure investigations, it was found that under the influence of projectile impact loading the cracking mechanism in composite materials is based on brittle cracking with the propagation path running mainly along the grain boundaries. In case of occurrence of areas with the absence of α-$Al_2O_3$ particles on the crack path, the crack front changes the direction of propagation and follows the border with these areas.

3. The presence of numerous microcracks, indicating the accumulation of stresses in these zones, was found in the vicinity of the main radial cracks. Deformations of the material in these areas cause regrouping of particles leading to brittle fracture, fragmentation of the material, and delamination at the warp-reinforcement boundaries.

4. The proposed hybrid numerical method based on the combination of FEM and SPH enables the modeling of dynamic puncture processes of complex multi-component material systems such as composite ones. The merger of methods makes it possible to model systems combining a plastic matrix with a brittle phase added.

## Acknowledgment

The research was financially supported by grants for statutory activity no. 0401/0015/18 of the Wroclaw University of Science and Technology. Calculations have been carried out in Wroclaw Centre for Networking and Super-computing (http://www.wcss.pl), grant No. 452

## References

[1] Skaggs, S.R. (2003). A brief history of ceramic armor development. In M. Waltraud Kriven & Hua-Tay Lin (eds.), *14 Book Series: Ceramic Engineering and Science Proceedings*. DOI: 10.1002/9780470294802.ch51

[2] Swab, J.J. (2013). *Advances in ceramic armor VIII*. New Jersey: A. John Wiley &Sons Inc. Publ.

[3] Crouch, I.G. (2019). Body armour - New materials, new systems. *Defence Technology*. 15, 241-253. DOI: 10.1016/j.dt. 2019.02.002

[4] Swab, J.J., Sandoz-Rosado E.J. (2017). Identifying opportunities in the development of ceramic matrix composite (CMC) materials for armor applications. US Army Research Laboratory, Report No. ARL-TR-7987.

[5] Belyakov, A.V., Ivanov, D.A. & Fomina, G.A. (1997). A lanxide ceramic composite material. *Glass and Ceramics*. 54 (7-8), 212-214.

[6] Garshin, A.P., Kulik, V.I. & Nilov, A.S. (2012). Analysis of the status and prospects for the commercial use of fiber-reinforced silicon-carbide ceramics. *Refractories and Industrial Ceramics*. 53(1), 62-70. DOI: 10.1007/s11148-012-9463-9.

[7] Dolata, A.J., Dyzia, M. (2012). Aspects of fabrication aluminium matrix heterophase composites by suspension method. *IOP Conf. Series: Materials Science and Engineering*. 35 012020. DOI:10.1088/1757-899X/35/1/012020.

[8] Rawlings, R.D. (1994). Glass-ceramic matrix composites. *Composites*. 25(5), 372-379.

[9] Danko, G.A., Popović, D. & Stuffle, K. (1995). Commercial development of fibrous monolithic ceramics. *Ceramic Engineering and Science Proceedings*. 16(5), 673-680.

[10] Kurzawa, A., Pyka, D., Jamroziak, K., Bocian, M., Kotowski, P. & Widomski P. (2018). Analysis of ballistic resistance of composites based on EN AC-44200 aluminum alloy reinforced with $Al_2O_3$ particles. *Composite Structures*. 201, 834-844.

[11] Kurzawa, A., Bocian, M., Jamroziak, K., Pyka, D. (2018). Analysis of ceramic-metallic composites of ballistic resistance on shots by 5.56 mm ammunition. In 23rd Proceedings International Conference on Engineering Mechanics, 15-18 May 2017 (pp. 574-577). Svratka, Czech Republic: Brno University of Technology.

[12] Kurzawa, A., Pyka, D., Pach, A., Jamroziak, K. & Bocian, M. (2017). Numerical modeling of the microstructure of ceramic-metallic materials. *Procedia Engineering*. 199, 1459-1500.

[13] Heidenreich, B., Crippa, M., Voggenreiter, H., Strasburger, E., Gedon, H. & Nordmann, M. (2010). Development of biomorphic SiSiC- and C/SiSiC-materials for lightweight armour. *Ceramic Engineering and Science Proceedings*. 31, 207-220.

[14] Wang, S.X., Lan, H.F., Wang, W.J., Huang, Y.J. & Li, S.J. (2019). The influence of casting-calendering process on the microstructure of pure $Al_2O_3$ ceramic substrate. *Ceramic Engineering and Science Proceedings*. 39(1), 15-22.

[15] Gawdzinska, K., Nagolska, D. & Szymanski, P. (2018) Determination of Duration and Sequence of Vacuum Pressure Saturation in Infiltrated MMC Castings. *Archives of Foundry Engineering.* 18(1), 23-28.

[16] Kılıc, N. & Ekici, B. (2013). Ballistic resistance of high hardness armor steels against 7.62 mm armor piercing ammunition. *Materials and Desing*. 44, 35-48.

[17] Mazurkiewicz, L., Malachowski, J. & Baranowski, P. (2015). Optimization of protective panel for critical supporting elements. *Composite Structures*. 134, 493-505.

[18] Murugesan, M. & Jung, D.J. (2019). Johnson Cook material and failure model parameters estimation of AISI-1045 medium carbon steel for metal forming applications. *Materials*. 12, 609. DOI:10.3390/ma12040609.

[19] Murugesan, M., Lee, S., Kim, D., Kang, Y.H. & Kim, N. (2017). A comparative study of ductile damage models approaches for joint strength prediction in hot shear joining process. *Procedia Engineering*. 207, 1689-1694.

[20] Gasiorek, D., Baranowski, P., Malachowski, J., Mazurkiewicz, L. & Wiercigroch, M. (2018). Modelling of guillotine cutting of multi-layered aluminum sheets. *Journal of Manufacturing Processes*. 34, 374-388.

[21] Baranowski, P., Janiszewski, J. & Malachowski, J. (2014). Study on computational methods applied to modeling of pulse shaper in split-Hopkinson bar. *Archives of Mechanics*. 66(6), 429-452.

[22] Baranowski, P., Gieleta, R., Malachowski, J., Damaziak, K. & Mazurkiewicz, L. (2014). Split Hopkinson Pressure Bar impulse experimental measurement with numerical validation. *Metrology and Measurement Systems*. 21(1), 47-58.

[23] Kucewicz, M., Baranowski, P., Malachowski, J., Trzcinski, W., Szymanczyk, L. (2019). Numerical modelling of cylindrical test for determining jones – Wilkins - Lee equation parameters. In E. Rusinski & D. Pietrusiak (Eds.), Lecture Notes in Mechanical Engineering (pp. 388-394). Springer, Cham, Switzerland.